# Squeezing the fundamental temperature fluctuations of a high-Q microresonator

Xuan Sun, Rui Luo, Xi-Cheng Zhang, and Qiang Lin

Phys. Rev. A **95**, 023822 — Published 10 February 2017

DOI: 10.1103/PhysRevA.95.023822

# Squeezing the Fundamental Temperature Fluctuations of A High-Q Micro/Nanoresonator

Xuan Sun,[1] Rui Luo,[1] Xi-Cheng Zhang,[1] and Qiang Lin[1,2,*]

[1]*Institute of Optics, University of Rochester, Rochester, NY 14627*

[2]*Department of Electrical and Computer Engineering, University of Rochester, Rochester, NY 14627*

Temperature fluctuations of an optical resonator underlie a fundamental limit of its cavity stability. Here we show that the fundamental temperature fluctuations of a high-Q micro/nanoresonator can be suppressed remarkably by pure optical means without cooling the device temperature. An optical wave launched into the cavity is able to produce strong photothermal backaction which dramatically suppresses the spectral intensity of temperature fluctuations and squeezes its overall level by orders of magnitude. The proposed photothermal temperature squeezing is expected to significantly improve the stability of optical resonances, with potentially profound impact on broad applications of high-Q cavities in sensing, metrology, and nonlinear/quantum optics.

## I. INTRODUCTION

Thermal fluctuations are fundamental thermodynamical phenomena in physical systems, which manifest as noise sources in many applications. In the context of high-quality (high-Q) optical resonators, thermal fluctuations in physical dimensions (thermal mechanical), thermal expansion (thermo-elastic), and refractive index (thermo-refractive) impose fundamental limits on the stability of optical cavity resonances [1–3] which impact many important applications such as laser frequency stabilization [3], precision measurement [4], quantum optics [5], and diverse optical sensing [6–8]. In recent years, significant efforts have been devoted to developing various approaches to actively suppress the thermal mechanical noises by cooling the effective temperature of the underlying mechanical mode [9]. The active control of thermo-elastic and thermo-refractive noises, however, have been left largely intact, the latter of which plays a dominant role in microscopic optical resonators due to the significantly reduced physical sizes of devices [6–8, 10–12].

Here we show that the fundamental temperature fluctuations and the resulting thermo-refractive noises of a high-Q micro/nanoresonator can be dramatically squeezed by an optical wave launched into the cavity. In contrast to thermal mechanical noise, this can be achieved remarkably without cooling the device temperature. The underlying physical mechanism is the photothermal backaction between the device temperature and the intracavity optical energy, as schematically shown in Fig. 1. For an optical wave launched into the cavity, a small fraction of the energy would be absorbed by the device material and converted into heat. The temperature fluctuations of the device modulate the resonance frequency of the cavity, which in turn perturbs the intracavity energy. Consequently, the magnitude of photothermal heating changes accordingly which eventually back-acts onto the device temperature itself. Such a photothermal backaction mechanism underlies various thermo-optic nonlinear phenomena that have attracted considerable interest recently [5, 13–27]. However, its intriguing interaction with the fundamental thermo-optic noises of a high-Q resonator has been neglected in the past explorations [1–27]. As we will show below, photothermal backaction exhibits very profound impact on the characteristics of the fundamental temperature fluctuations, squeezing its amplitude and the resulting thermo-refractive noises by orders of magnitudes.

## II. TEMPERATURE SQUEEZING

For a distribution of temperature fluctuation $\Delta T(\boldsymbol{r},t)$ across a monolithic optical micro/nanoresonator, the thermo-optic effect results in a shift of the optical cavity resonance $\omega_0$ by an amount of $\delta\omega(T) \equiv g_T \Delta\bar{T}$, where $g_T \equiv \frac{d\omega_0}{dT} = -\frac{\omega_0}{n}\frac{dn}{dT}$ stands for the photothermal coupling coefficient and $\frac{dn}{dT}$ is the thermo-optic coefficient of the device material [10]. $\Delta\bar{T}$ is the device temperature variation averaged over the optical mode field profile (Appendix A). Consequently, the optical field inside the cavity is described by the following equation

$$\frac{da}{dt} = (i\Delta_0 - \Gamma_t/2)a - ig_T\Delta\bar{T}a + i\sqrt{\Gamma_e}A, \qquad (1)$$

where $\Delta_0 = \omega_l - \omega_0$ is the detuning of the laser frequency $\omega_l$ to the cavity resonance $\omega_0$. $\Gamma_t$ and $\Gamma_e$ are the photon decay rate

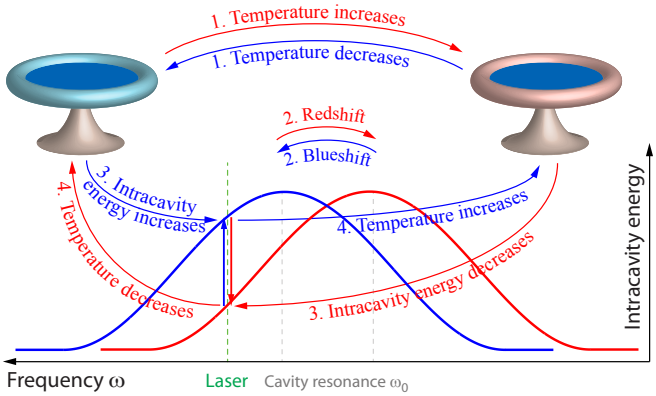


FIG. 1: Schematic of photothermal backaction to squeeze the temperature fluctuation of a device (shown as a microtoroid). A variation of device temperature (1) shifts the resonance frequency of the cavity (2) (assuming $\frac{dn}{dT} > 0$), resulting in a perturbation to the intracavity optical energy (3). As a result, the magnitude of photothermal heating changes, which in turn leads to a backaction on the device temperature (4).

*Electronic address: qiang.lin@rochester.edu

and external coupling rate, respectively, of the loaded cavity, with a corresponding optical Q given by $Q_t = \omega_0/\Gamma_t$. $a$ and $A$ are the amplitudes of the intracavity field and the input field, respectively, normalized such that $|a|^2$ and $|A|^2$ represent the intracavity energy and the input power, respectively.

The dynamics of the device temperature variation $\Delta T(\boldsymbol{r},t)$ is governed by the equation of thermal diffusion [1, 2, 10, 13]. Averaging it over the optical mode field, we can find that the mode-averaged temperature fluctuation $\Delta\bar{T}$ satisfies the following equation (Appendix B)

$$\frac{d(\Delta\bar{T})}{dt} = -\Gamma_T \Delta\bar{T} + \eta_T |a|^2 + \xi(t), \tag{2}$$

where $\Gamma_T$ represents the thermal relaxation rate which is related to the thermal diffusivity of the device, and $\eta_T$ is the photothermal heating coefficient that is related to the optical absorption and heat conversion [10, 13] (see also Appendix B). $\xi(t)$ describes the thermal fluctuation source with the following characteristics

$$\langle \xi(t)\xi(t+\tau)\rangle = \frac{2\Gamma_T k_B T_0^2}{\rho C V}\delta(\tau), \tag{3}$$

where $\rho$ is the material density, $C$ is the specific heat capacity, $V$ is the effective mode volume, $k_B$ is the Boltzmann constant, and $T_0$ is the device temperature at thermal equilibrium. $\delta(\tau)$ is the Dirac delta function.

In the absence of the optical absorption, Eq. (2) together with Eq. (3) results in a temperature fluctuation as $\langle(\delta\bar{T})^2\rangle_0 = \frac{k_B T_0^2}{\rho C V}$, which is expected from the fluctuation-dissipation of the system [1, 2, 10, 28]. This temperature fluctuation leads to a fundamental uncertainty of cavity resonance $\langle(\delta\omega)^2\rangle_0 = g_T^2\langle(\delta\bar{T})^2\rangle_0$ which imposes fundamental thermo-refractive noise on the cavity resonance [1, 2, 10, 11]. On the other hand, without the noise term $\xi(t)$, Eqs. (1) and (2) lead to the well-known thermo-optic nonlinearity that has been extensively explored in recent years [5, 13–27]. For example, a continuous-wave (CW) laser launched into the cavity at a detuning of $\Delta_0$ would result in a static temperature rise of $\Delta\bar{T}_0 = \frac{\eta_T|a_0|^2}{\Gamma_T}$ which changes the laser-cavity detuning to $\Delta_0' = \Delta_0 - g_T\Delta\bar{T}_0$ and thus in turn modifies the intracavity energy to be $U_o \equiv |a_0|^2 = \frac{\Gamma_e|A|^2}{(\Delta')^2+(\Gamma_t/2)^2}$ where $|A|^2$ is the input optical power. A stable thermo-optic locking appears when $g_T$ and $\Delta_0'$ have opposite signs (say, a blue laser-cavity detuning, $\Delta_0' > 0$, in a device with $\frac{dn}{dT} > 0$), which helps stabilize the laser-cavity detuning [14] and reduce the coupling of laser frequency noises [22].

The situation becomes very interesting in the presence of both thermal noises and thermo-optic nonlinearity, where the photothermal backaction would dramatically modify the characteristics of thermal fluctuations. As the temperature variation consists of both the fundamental thermal fluctuations and the static temperature rise induced by photothermal heating, it can be written as $\Delta\bar{T} = \Delta\bar{T}_0 + \delta\bar{T}(t)$. Accordingly, the cavity field becomes $a = a_0 + \delta a(t)$ where $a_0$ is the cavity field under the impact of static temperature rise $\Delta\bar{T}_0$, as described above in the previous paragraph, and $\delta a(t)$ represents the field fluctuation induced by the temperature fluctuations. From Eqs. (1) and (2), we can find $\delta\bar{T}$ and $\delta a$ are governed by the following equations

$$\frac{d(\delta a)}{dt} = (i\Delta_0' - \Gamma_t/2)\delta a - ig_T a_0 \delta\bar{T}, \tag{4}$$

$$\frac{d(\delta\bar{T})}{dt} = -\Gamma_T\delta\bar{T} + \eta_T(a_0^*\delta a + a_0\delta a^*) + \xi(t). \tag{5}$$

Equations (4) and (5) can be solved analytically to find the spectral intensity of the temperature fluctuation. In general, the thermal relaxation rate is much smaller compared with the photon decay rate of the optical cavity. As a result, the spectral intensity of the temperature fluctuations is given by a simple expression as (Appendix C)

$$S_{\delta\bar{T}}(\Omega) = \frac{2\Gamma_T k_B}{\rho C V}\frac{\left(T_0 + \frac{\eta_T}{\Gamma_T}|a_0|^2\right)^2}{(\Gamma_T')^2 + (\kappa_T\Omega)^2}, \tag{6}$$

where $\Gamma_T'$ and $\kappa_T$ are given by

$$\Gamma_T' = \Gamma_T - \frac{2\eta_T g_T |a_0|^2 \Delta_0'}{(\Delta_0')^2 + (\Gamma_t/2)^2}, \tag{7}$$

$$\kappa_T = 1 + \frac{2\eta_T g_T |a_0|^2 \Gamma_t \Delta_0'}{[(\Delta_0')^2 + (\Gamma_t/2)^2]^2}. \tag{8}$$

In the absence of photothermal backaction, Eq. (6) reduces to the case of a passive cavity, with a peak value of $S_0 = \frac{2k_B T_0^2}{\rho C V \Gamma_T}$.

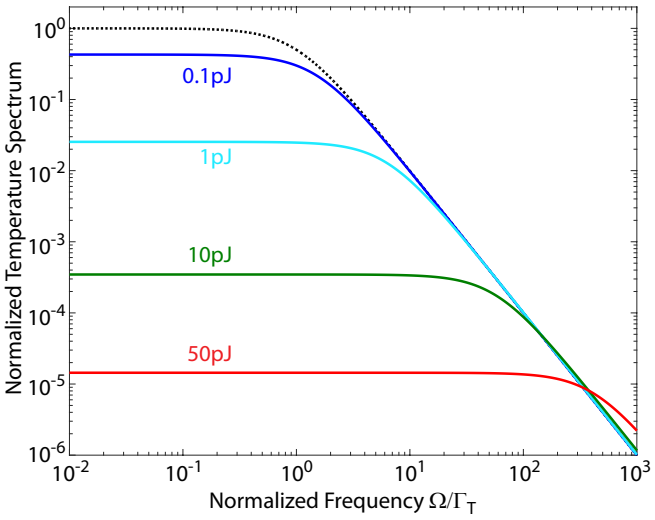


FIG. 2: Spectral intensity of temperature fluctuation, normalized by $S_0 = \frac{2k_B T_0^2}{\rho C V \Gamma_T}$ of a passive cavity. The dashed curve shows the case in the absence of optical wave. The device is assumed to be a silica microtoroid at room temperature of $T_0 = 300$ K, with $\Gamma_T = 90$ kHz, $\eta_T = 2.87\times10^{15}$ K/(J·s), $\frac{dn}{dT} = 1.2\times10^{-5}$ K$^{-1}$, density $\rho = 2200$ Kg/m$^3$, and effective mode volume $V = 5\times10^{-16}$ m$^3$. All these parameters are from Ref. [18]. The device is assumed to have an optical Q of $10^7$ for the loaded cavity. The laser frequency is located in the telecom band, with an optimal laser-cavity detuning of $\Delta_0' = \Gamma_t/2$.

Detailed analysis shows that $\kappa_T$ characterizes different regimes of photothermal backaction. When $\kappa_T < 0$, the photothermal backaction excites the temperature variation into unstable regime, leading to dynamic thermo-optic oscillation. Therefore, $\kappa_T = 0$ sets the maximal optical energy of $|a_0|^2_{\max} = -\frac{[(\Delta_0')^2+(\Gamma_t/2)^2]^2}{2\eta_T g_T \Gamma_t \Delta_0'}$ below which the resonator remains stable. In this regime, Eq. (7) shows that photothermal backaction modifies the effective thermal relaxation rate, with a sign dependent on the laser-cavity detuning. The effective thermal relaxation rate increases on one side of laser-cavity detuning, *e.g.*, $\Delta_0' > 0$ for $\frac{dn}{dT} > 0$ ($\Delta_0' < 0$ for $\frac{dn}{dT} < 0$), with a magnitude dependent on the optical energy. For a given optical energy, the effect of photothermal backaction is maximized with a laser-cavity detuning of $\Delta_0' = \Gamma_t/2$ (for $\frac{dn}{dT} > 0$. $\Delta_0' = -\Gamma_t/2$ for $\frac{dn}{dT} < 0$), leading to $\Gamma_T' = \Gamma_T + 2\eta_T |g_T||a_0|^2/\Gamma_t$ and $\kappa_T = 1 - 4\eta_T |g_T||a_0|^2/\Gamma_t^2$. Consequently, the amplitude of the temperature spectral intensity would be significantly reduced. In the following, we focus on the effect for devices at room temperature, since a majority of applications operate at this temperature. We will use a high-Q silica microtoroid [29] as a typical example to show the related phenomena.

Figure 2 shows the spectral intensities of temperature fluctuation inside a silica microtoroid with an optical Q of $10^7$, normalized by the peak value of $S_0 = \frac{2k_B T_0^2}{\rho C V \Gamma_T}$ for a passive cavity in the absence of photothermal backaction. It shows clearly that the spectral amplitude of temperature fluctuations decreases dramatically with increased optical energy, while the spectral width increases accordingly at the same time. At low frequencies, $S_{\delta\bar{T}}(\Omega)|_{\Omega\approx 0} = 3.38 \times 10^{-14}$ K$^2$/Hz for the passive device at room temperature. However, with the photothermal backaction, $S_{\delta\bar{T}}(\Omega)|_{\Omega\approx 0}$ is suppressed by nearly five orders of magnitude, to a value of $4.87 \times 10^{-19}$ K$^2$/Hz, with an optical energy of 50 pJ. This energy corresponds to an optical power of only about 6.3 mW launched into the cavity assuming the microresonator is critically coupled, clearly showing the powerfulness of suppressing the temperature fluctuations by photothermal backaction.

For many practical sensing applications such as sensing biomolecules [7, 8], electromagnetic field [30], gas [31], mechanical acceleration [32], rotation [33], diffusion kinetics [34], etc, the temperature fluctuation spectrum at low frequencies around DC are most relevant since the signals under detection vary slowly with time, where the thermo-refractive noise of the device becomes a fundamental limiting factor [6, 35–37]. Here we show that the photothermal backaction is able to significantly improve the sensing resolution by orders of magnitude compared with the fundamental thermodynamic limit of a passive cavity. Similarly, it might be able to improve considerably the long-term drift if a high-Q microresonator is used to for laser frequency stabilization [11, 12, 38].

The variance of the temperature fluctuations can be obtained by integrating Eq. (6) over frequency, which is given by

$$\langle(\delta\bar{T})^2\rangle = \frac{\Gamma_T}{\kappa_T \Gamma_T'} \frac{k_B T_0^2}{\rho C V} \left(1 + \frac{\eta_T |a_0|^2}{\Gamma_T T_0}\right)^2. \qquad (9)$$

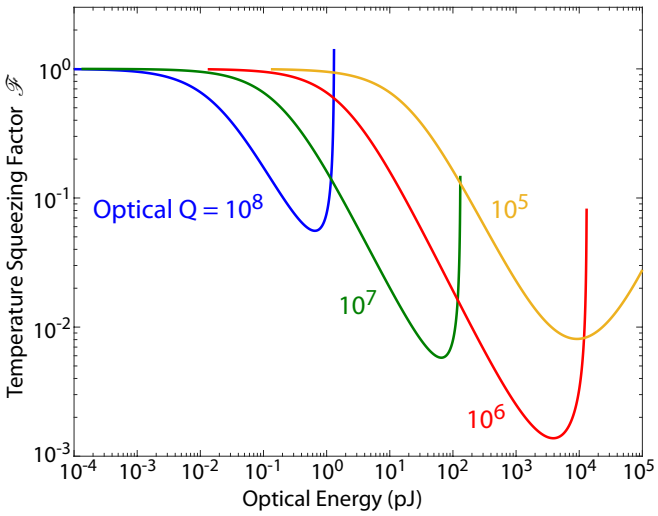


FIG. 3: Temperature squeezing factor as a function of optical energy inside the cavity, for the example of silica microtoroid given in the caption of Fig. 2.

In the absence of photothermal effect, Eq. (9) reduces to $\langle(\delta\bar{T})^2\rangle_0 = \frac{k_B T_0^2}{\rho C V}$, as expected for a passive cavity. The photothermal effect has two impacts on the temperature fluctuations. On one hand, the photothermal backaction on the device temperature produces negative feedback to suppress its fluctuations by a factor of $\frac{\Gamma_T}{\kappa_T \Gamma_T'}$. On the other hand, the photothermal heating would raise the device temperature to $\bar{T} = T_0 + \frac{\eta_T |a_0|^2}{\Gamma_T}$, which in turn would lead to an increase of temperature fluctuation. These two competing effects combines together, resulting in the overall level of temperature fluctuations given in Eq. (9). It is important to note that the suppression of the temperature fluctuations is realized here without cooling the device temperature. In fact, the device temperature increases by a certain amount due to the photothermal heating. In this sense, the photothermal backaction *squeezes* the device temperature towards its mean value, rather than cooling it as what is generally done in suppressing thermal mechanical noise [9]. On the other hand, the photothermal backaction squeezes the temperature fluctuations primarily at the locations where the optical mode field is distributed. Other portion of the device is not relevant to the photothermal interaction.

For convenience, we define a temperature squeezing factor as $\mathscr{F} \equiv \frac{\langle(\delta\bar{T})^2\rangle}{\langle(\delta\bar{T})^2\rangle_0}$, which characterizes the relative magnitude of temperature fluctuation under the impact of photothermal backaction, in comparison with that of a passive resonator. Figure 3 shows the squeezing factor for a silica microtoroid. In general, the temperature fluctuation decreases quickly with increased optical energy because of increased photothermal backaction. It reaches a minimum value at a certain optical energy beyond which the impact from static temperature rise starts to dominate, resulting in an increase of temperature fluctuations. When the optical Q is $10^8$, the squeezing factor reaches a minimum value of 0.055 with an optical energy of

0.65 pJ. However, the minimum value decreases dramatically to 0.0014 when the optical Q becomes $10^6$, while a higher optical energy of 3.8 nJ is required to provide enough strength of photothermal backaction.

Figure 3 shows that, for a device with a certain optical Q, there exists an optical energy that produces the optimal temperature squeezing. From Eq. (9), we can find that the optimal value of the squeezing factor is given by (Appendix D)

$$\mathscr{F}_o = \frac{8\Gamma_T}{\Gamma_t} + \frac{2\Gamma_t}{|g_T|T_0} = \frac{8\Gamma_T Q_t}{\omega_0} + \frac{2n}{|\frac{dn}{dT}|T_0 Q_t}, \tag{10}$$

which is achieved with an optical energy of

$$|a_0|^2 = \frac{\Gamma_T T_0/\eta_T}{1+8|g_T|T_0\Gamma_T/\Gamma_t^2}. \tag{11}$$

This value of optical energy is always below the onset of thermo-optic oscillation, $|a_0|^2_{\max}$. Therefore, in principle, the optimal temperature squeezing can always be realized in the stable thermo-optic locking regime.

It is interesting to note that high optical Q does not necessarily indicate an improvement on the temperature squeezing. Equation (10) shows that the maximum temperature squeezing is given by

$$\mathscr{F}_m = 8\sqrt{\frac{\Gamma_T}{|g_T|T_0}}, \tag{12}$$

which is achieved at an optical Q and required optical energy as

$$Q_t = \frac{\omega_0}{2\sqrt{\Gamma_T|g_T|T_0}}, \qquad |a_0|^2 = \frac{\Gamma_T T_0}{3\eta_T}. \tag{13}$$

Interestingly, the maximum temperature squeezing and the corresponding required optical Q depends only on the thermal relaxation rate and the photothermal coupling coefficient, but independent of the photothermal heating efficiency. The latter only affects the required optical energy.

In general, optical materials exhibit thermo-optic coefficients $|\frac{dn}{dT}| \sim (10^{-6}-10^{-4})$ at room temperature [39]. The thermal relaxation rate of a micro/nano-photonic resonator, however, varies considerably with the device structure and material. Equation (12) shows that the maximum squeezing factor can be as large as $\mathscr{F}_m \sim 10^{-4}-10^{-3}$ for a thermal relaxation rate in the range $\Gamma_T \sim (1-100)$ kHz that exist in current devices [10–27]. It corresponds to a root-mean-square value of $\sqrt{\mathscr{F}_m} \sim 0.01-0.03$. In general, a monolithic microresonator exhibits an intrinsic temperature fluctuation [12] in the order of $\sqrt{\langle(\delta\bar{T})^2\rangle_0} \sim 1\ \mu$K at room temperature, corresponding to a resonance stability in the order of $\frac{\sqrt{\langle(\delta\omega)^2\rangle_0}}{\omega_0} \sim 10^{-12}$. We expect that the photothermal backaction is able to squeeze them down to as small as $\sqrt{\langle(\delta\bar{T})^2\rangle} \sim 10$ nK and $\frac{\sqrt{\langle(\delta\omega)^2\rangle}}{\omega_0} \sim 10^{-14}$. The corresponding required optical Q is $\sim 10^6-10^7$, which is readily available for many device platforms. Equation (12) indicates that a small thermal relaxation rate is desired to achieve large temperature squeezing. In practice, this can be achieved by optimizing device structure design to engineer the heat transport [40].

## III. IMPACT OF LASER NOISES

The discussions in the previous section focus on the classical regime assuming a constant power of the input CW laser. However, a CW laser inevitably exhibits certain fluctuations on its intensity due to the quantum nature of light. Such quantum fluctuations of laser intensity would produce quantum backaction to the temperature fluctuations. On the other hand, a practical CW laser is accompanied with certain amount of intensity and frequency noises. These noises would perturb the optical energy inside the cavity and thus introduce extra photothermal fluctuations on device temperature. We investigate in this section the impacts of these classical and quantum fluctuation of the laser.

Detailed analysis (Appendix E) shows that the spectral intensity of temperature fluctuations is described by the following expression similar to Eq. (6):

$$S_{\delta\bar{T}}(\Omega) = \frac{S_\xi + S_Q + S_L}{(\Gamma_T')^2 + (\kappa_T\Omega)^2}, \tag{14}$$

where $\Gamma_T'$ and $\kappa_T$ are given by Eqs. (7) and (8). In Eq. (14), $S_\xi$ describes the effect of photothermal heating, which is given by (see also Appendix C)

$$S_\xi = \frac{2\Gamma_T k_B}{\rho C V}\left(T_0 + \frac{\eta_T}{\Gamma_T}U_o\right)^2, \tag{15}$$

where $U_o$ is the optical energy inside the cavity as given in the previous section. $S_Q$ describes the effect of quantum backaction from the quantum fluctuations of the input laser, which is given by

$$S_Q(\Omega) = \frac{\eta_T^2\hbar\omega_0 U_o\Gamma_t}{(\Delta_0')^2 + (\Gamma_t/2)^2}. \tag{16}$$

$S_L$ describes the effect of the classical noises accompanied with the input laser, which is given by

$$S_L(\Omega) = \eta_T^2 U_o^2\left\{S_{\rm RIN}(\Omega) + \frac{(2\Delta_0')^2 S_\omega(\Omega)}{[(\Delta_0')^2 + (\Gamma_t/2)^2]^2}\right\}, \tag{17}$$

where $S_{\rm RIN}(\Omega)$ and $S_\omega(\Omega)$ are the spectral densities of laser relative intensity noise and frequency noise, respectively (see Appendix E for detailed discussions).

Equations (14)-(17) provide a complete description of the temperature spectrum under the impact of photothermal backaction, quantum backaction, and the laser classical noises. As shown in Eq. (14), these three contributions to the temperature fluctuations are determined by the relative magnitude of $S_\xi$, $S_Q$, and $S_L$. In the following, we provide an estimate of the relative magnitude of these contributions.

**Effect of quantum backaction:** Detailed analysis shows that the impact of quantum backaction is negligible when the device is at room temperature. Figure 4a compares the relative magnitude of $S_Q$ with $S_\xi$, for the example of a high-Q silica microtoroid [18]. As shown in Fig. 4a, for a normal optical energy below the onset of thermo-optic oscillation, $S_Q$ is at least two orders of magnitude smaller than $S_\xi$ for a device

at room temperature. Figure 4b shows the temperature dependence of $\frac{S_Q}{S_\xi}$, with an optical energy given in Eq. (11) that achieves the optimal temperature squeezing. It shows clearly that the impact of quantum backaction is negligible until the device temperature becomes below 10K.

**Effect of laser classical noises:** Figure 5 and 6 show the impact of laser intensity and frequency noises, respectively. In general, laser intensity and frequency noises introduces extra photothermal heating with a magnitude dependent quadratically on the intracavity energy (Eq. (17)). Therefore, their impacts are small at low optical energy but can become considerable when the optical energy increases to large values. As a result, the optimal point of temperature squeezing shifts to lower optical energy, with a reduced squeezing magnitude. Semiconductor diode lasers generally exhibit a low level of relative intensity noise in the range of $\sim(-160--150)$ dB/Hz in the spectral range well below the relaxation frequency [41]. Figure 5b shows that its impact on the temperature squeezing is relatively small, with an optimal temperature squeezing factor still as large as $\mathscr{F}_o = 0.007 - 0.02$. Similar temperature squeezing can be obtained with laser frequency noises in the range of $(10^2 - 10^3)$ Hz$^2$/Hz (Fig. 6b). Such level of laser frequency noises is available in frequency-stabilized semiconductor lasers [42–50], some of which are commercially available [51]. Therefore, we expect that significant temperature squeezing can be achieved experimentally with these types of semiconductor lasers.

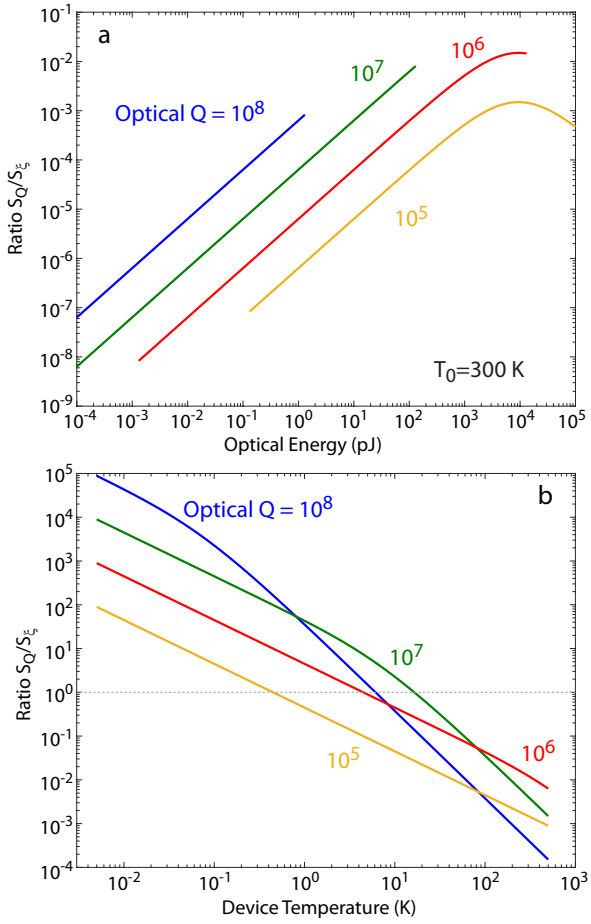


FIG. 4: Impact of quantum backaction on temperature squeezing. **a.** $\frac{S_Q}{S_\xi}$ as a function of optical energy inside the cavity. The device is at room temperature $T_0 = 300$ K. **b.** $\frac{S_Q}{S_\xi}$ as a function of device temperature, with an optical energy given in Eq. (11) that achieves the optimal temperature squeezing. The device parameters are given in the caption of Fig. 2.

## IV. ON THE THERMO-ELASTIC EFFECT

The discussions above focus on the temperature squeezing related to the thermo-refractive effect. It is straightforward to show that the same idea applies to the effect induced by thermal expansion (thermo-elastic effect) as well, since photothermal backaction via the thermo-elastic coupling functions in a similar fashion as that via thermo-optic coupling, while the former involves device geometry variation rather than refractive index change in the latter (see Appendix F for some detailed discussions). Therefore, we expect that the photother-

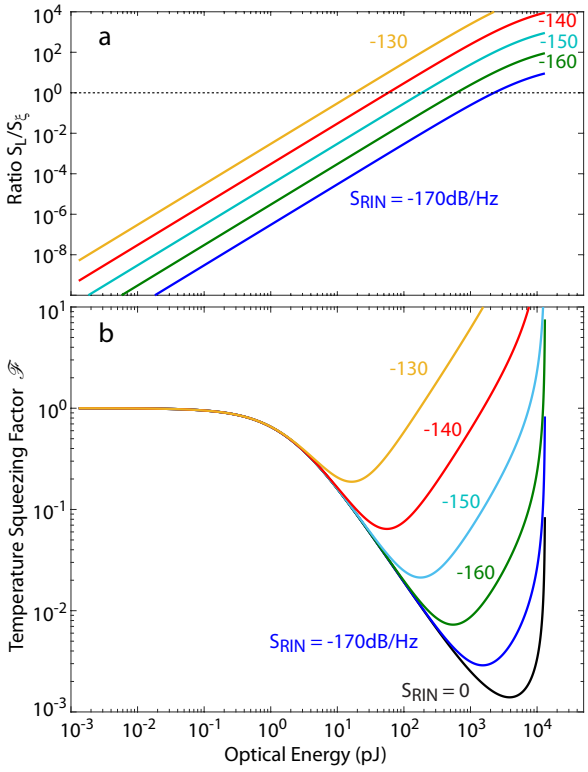


FIG. 5: Impact of laser intensity noises on temperature squeezing. **a.** $\frac{S_L}{S_\xi}$ as a function of optical energy inside the cavity. **b.** Temperature squeezing factor. In **b**, quantum backaction is included as well, but it has negligible effect. The black curves show the case in the absence of laser intensity noises, as a reference. To simplify the analysis, we assume a frequency independent $S_{\rm RIN}(\Omega)$ in **(b)**. The device is assumed to be a silica microtoroid at room temperature $T_0 = 300$ K, with an optical Q of $10^6$. Other parameters are the same as Fig. 4.

mal temperature squeezing would behave in a similar manner for the thermo-elastic effect.

In general, temperature squeezing occurs in a device with either dominant thermo-refractive, dominant thermo-elastic effect, or comparable thermo-refractive and thermo-elastic effects that act constructively on the optical cavity resonance. However, the situation becomes complicated if the two effects are comparable with each other but counteract with each other. In this case, the resonator can become unstable with dynamic oscillation, as shown in Ref. [18, 20, 21, 25–27]. Although the dynamics of static temperature variation is well studied [18, 20, 21, 25–27], it is not clear how the temperature fluctuations are impacted in this case, which will be left for future exploration.

## V. ON THE EXPERIMENTAL CHARACTERIZATION

The temperature fluctuations of the device perturb the cavity resonance, which will be transduced to the fluctuations of the optical power transmitted from the cavity. As the transmitted optical power is $P_o = |A + i\sqrt{\Gamma_e}a|^2 = |A + i\sqrt{\Gamma_e}(a_0 + \delta a)|^2$, the induced power fluctuation is thus given by $\delta P_o(t) = i\sqrt{\Gamma_e}[A_t^* \delta a(t) - A_t \delta a^*(t)]$, where $A_t \equiv A + i\sqrt{\Gamma_e}a_0$ is the transmitted optical field in the absence of temperature fluctuations, $a_o$ is given by Eq. (C3), and $\delta a$ is governed by Eq. (4). From Eqs. (1), (4), and (5), we can find the spectral intensity of the power fluctuations is given by the following expression:

$$S_{\delta P_o}(\Omega) = g_T^2 S_{\delta\bar{T}}(\Omega) H(\Delta_0'), \tag{18}$$

where $H(\Delta_0')$ is the cavity transduction function with the following form

$$H(\Delta_0') = \frac{(2\Gamma_0\Gamma_e P\Delta_0')^2}{[(\Gamma_t/2)^2 + (\Delta_0')^2]^4}, \tag{19}$$

where $P$ is the input optical power and $\Gamma_0$ is the photon decay rate of the intrinsic cavity (see Appendix E, for example). To obtain Eq. (19), we have assumed that the thermal relaxation rate is much smaller than the photon decay rate of the cavity.

Therefore, as shown in Eq. (18), the temperature fluctuations of the device can be experimentally characterized by the power fluctuations on the cavity transmission. We thus propose an experimental scheme, as shown in Fig. 7, to measure the temperature squeezing. A strong pump laser is launched into a cavity mode of the high-Q resonator to produce temperature squeezing. At the same time, a weak probe laser is launched into a separate cavity mode (within the same mode family of the pump mode) to detect the induced temperature squeezing. Both lasers are locked to stabilized reference cavities (or wavelength references) to avoid potential wavelength drifts. The environmental temperature of the microresonator is stabilized to avoid potential temperature drift. The power spectra of the pump and probe waves output from the resonator can be measured by optical detectors and an electrical spectrum analyzer. Such a testing scheme would provide detailed characterization of the temperature squeezing effect. In practice, one potential interference might come from the optomechanical oscillation excited by the intense pump wave [9]. As this effect depends sensitively on the quality factor of the mechanical mode, it can be easily quenched by introducing mechanical damping to the device.

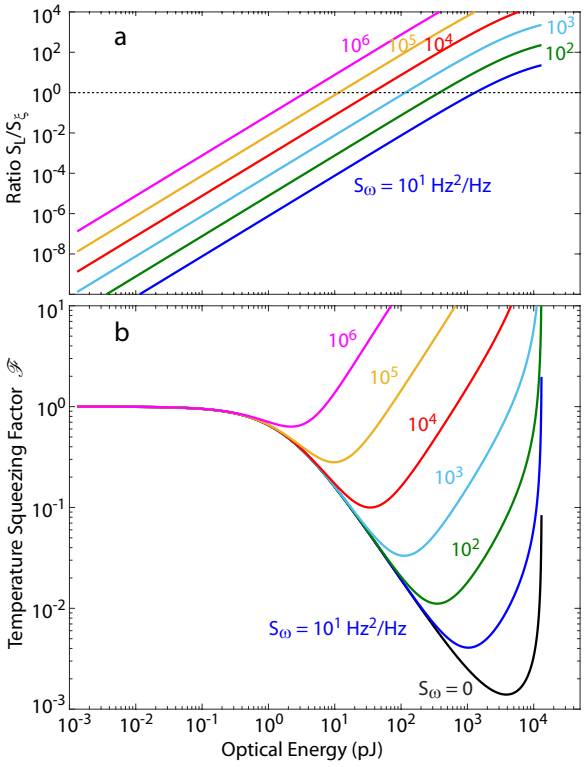


FIG. 6: Impact of laser frequency noises on temperature squeezing. **a.** $\frac{S_L}{S_\xi}$ as a function of optical energy inside the cavity. **b.** Temperature squeezing factor. In **b**, quantum backaction is included as well, but it has negligible effect. The black curves show the case in the absence of laser frequency noises, as a reference. To simplify the analysis, we assume a frequency independent $S_\omega(\Omega)$ in **(b)**. The device is assumed to be a silica microtoroid at room temperature $T_0 = 300$ K, with an optical Q of $10^6$. Other parameters are the same as Fig. 4.

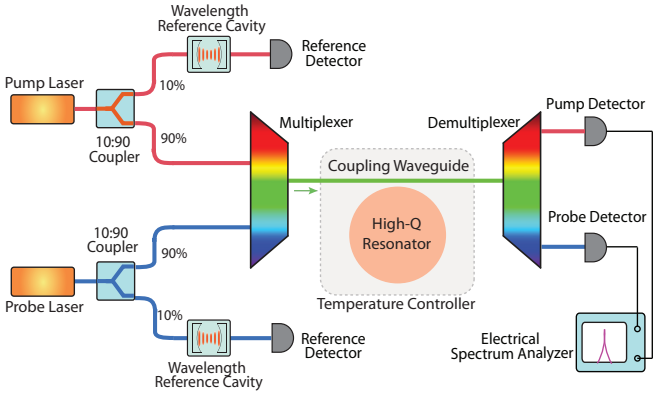


FIG. 7: Schematic of proposed experimental setup for characterizing the temperature squeezing.

## VI. CONCLUSION

In conclusion, we have shown by a simple theory that the fundamental temperature fluctuations of a high-Q micro/nanoresonator can be remarkably squeezed via the strong photothermal backaction from an optical wave launched into the cavity, without cooling the device temperature. For a device at room temperature, the spectral intensity of temperature fluctuations can be suppressed by five orders of magnitude and the overall level (RMS value) of temperature fluctuations can be squeezed by two orders of magnitude, resulting in a temperature fluctuation as small as $\sqrt{\langle(\delta\bar{T})^2\rangle} \sim 10$ nK achievable in a micro/nanoresonator. Such temperature squeezing would have profound impact on the application of optical micro/nanoresonators. To date, high-Q micro/nanoresonators have been applied for a vast variety of applications such as diverse sensing [6, 8], laser frequency stabilization [38], optical frequency comb generation and potential frequency synthesis [52], quantum squeezing [53], among many others. A majority of applications operate at room temperature and the fundamental temperature fluctuation of device is likely to be an ultimate limiting factor. The temperature squeezing proposed here offers an elegant solution to significantly reduce this impact, with great potential for realizing ultra-quiet micro/nanoresonators for broad applications.

## VII. ACKNOWLEDGEMENT

The authors thank Prof. Tao Lu at University of Victoria for helpful discussions. This work is supported in part by the Army Research Office grants (W911NF1410343 and W911NF1110297), the Defense Advanced Research Projects Agency under the QuASAR program, and the National Science Foundation under grants No. ECCS-1610674.

### Appendix A: Thermo-optic coupling and mode-averaged temperature variation

For a distribution of the temperature variation $\Delta T(\boldsymbol{r},t)$ across a monolithic optical resonator, the thermo-optic effect leads to a change of the dielectric function of the device material as $\Delta\varepsilon_r(\boldsymbol{r},T) = \frac{d\varepsilon_r}{dT}\Delta T(\boldsymbol{r},t) = 2n\frac{dn}{dT}\Delta T(\boldsymbol{r},t)$, where $n(\boldsymbol{r},T)$ is the refractive index and $\frac{dn}{dT}$ is the thermo-optic coefficient of the material. As a result, the cavity resonance $\omega_0$ is perturbed by an amount that can be obtained from the perturbation theory [54, 55] as

$$\delta\omega = -\frac{\omega_0}{2}\frac{\int \Delta\varepsilon_r|\boldsymbol{E}|^2 d^3\boldsymbol{r}}{\int \varepsilon_r|\boldsymbol{E}|^2 d^3\boldsymbol{r}} = -\frac{\omega_0}{n}\frac{dn}{dT}\frac{\int \varepsilon_r\Delta T|\boldsymbol{E}|^2 d^3\boldsymbol{r}}{\int \varepsilon_r|\boldsymbol{E}|^2 d^3\boldsymbol{r}}, \quad \text{(A1)}$$

where $\boldsymbol{E}(\boldsymbol{r})$ is the optical mode field and $\varepsilon_r(\boldsymbol{r})$ is the dielectric function of the device material. In the last expression of Eq. (A1), we have assumed the thermo-optic coefficient is uniform across the device. Equation (A1) shows clearly that the thermo-optic perturbation to the cavity resonance depends essentially on the temperature variation averaged over the optical mode field profile, $\delta\omega = g_T\Delta\bar{T}$, where the photothermal coupling coefficient is defined as $g_T \equiv \frac{d\omega_0}{dT} = -\frac{\omega_0}{n}\frac{dn}{dT}$ and the mode-averaged temperature variation is given by

$$\Delta\bar{T} \equiv \frac{\int \Delta T(\boldsymbol{r})\varepsilon_r|\boldsymbol{E}|^2 d^3\boldsymbol{r}}{\int \varepsilon_r|\boldsymbol{E}|^2 d^3\boldsymbol{r}}. \quad \text{(A2)}$$

The resulting cavity resonance under temperature perturbation is thus given by $\omega_0'(\bar{T}) = \omega_0 + \delta\omega = \omega_0 + g_T\Delta\bar{T}$. The dynamics of the optical field $a(t)$ inside the cavity is well described by the coupled mode theory [55, 56] as

$$\frac{da}{dt} = [i(\omega_l - \omega_0'(\bar{T})) - \Gamma_t/2]a + i\sqrt{\Gamma_e}A, \quad \text{(A3)}$$

where $\omega_l$ is the frequency of the input laser, $\Gamma_t$ and $\Gamma_e$ are the photon decay rate and external coupling rate, respectively, of the loaded cavity, with a corresponding optical Q given by $Q_t = \omega_0/\Gamma_t$. $a$ and $A$ are the amplitudes of the intracavity field and the input field, respectively, normalized such that $|a|^2$ and $|A|^2$ represent the intracavity energy and the input power, respectively. Substitute the expression of $\omega_0'$ into Eq. (A3), we obtain Eq. (1) in the main text.

### Appendix B: Dynamics of temperature fluctuations

The dynamics of the temperature fluctuations is governed by the equation of thermal diffusion as [1, 2, 10, 13]

$$\frac{\partial(\Delta T)}{\partial t} - D_T\nabla^2(\Delta T) = \frac{\alpha_T p_{\text{abs}}(\boldsymbol{r},t)}{C\rho} + F_T(\boldsymbol{r},t), \quad \text{(B1)}$$

where $D_T$, $C$, and $\rho$ are the thermal diffusivity, specific heat capacity, and density of the device material, respectively. $F_T(\boldsymbol{r},t)$ is the Langevin source of thermal fluctuations. $p_{\text{abs}}$ is the optical power density absorbed by the device material and $\alpha_T$ is the fraction of the absorbed power that is converted into heat. $p_{\text{abs}}$ is given as

$$p_{\text{abs}}(\boldsymbol{r},t) = \Gamma_a\frac{\varepsilon_0\varepsilon_r(\boldsymbol{r})}{2}|a(t)|^2|\boldsymbol{E}(\boldsymbol{r})|^2, \quad \text{(B2)}$$

where $\Gamma_a$ is the absorption rate of optical energy by the device material and $a(t)$ is the intracavity field amplitude normalized such that $|a(t)|^2$ represents the optical energy inside the cavity.

As shown in the previous section, what matters the optical field inside the cavity is the mode-averaged temperature fluctuations. Substitute Eq. (B2) into Eq. (B1) and integrate it over the optical mode profile, we find that the mode-averaged temperature variation satisfies the following equation

$$\frac{\partial(\Delta\bar{T})}{\partial t} - \frac{\int D_T\nabla^2(\Delta T)\varepsilon_r|\boldsymbol{E}|^2 d^3\boldsymbol{r}}{\int \varepsilon_r|\boldsymbol{E}|^2 d^3\boldsymbol{r}} = \eta_T|a(t)|^2 + \xi(t), \quad \text{(B3)}$$

where $\eta_T$ is the photothermal heating coefficient defined as

$$\eta_T \equiv \frac{\alpha_T\Gamma_a\varepsilon_0}{2C\rho}\frac{\int \varepsilon_r^2|\boldsymbol{E}|^4 d^3\boldsymbol{r}}{\int \varepsilon_r|\boldsymbol{E}|^2 d^3\boldsymbol{r}}, \quad \text{(B4)}$$

and $\xi(t)$ is the mode-averaged Langevin thermal source given as

$$\xi(t) \equiv \frac{\int \varepsilon_r F_T(\boldsymbol{r},t)|\boldsymbol{E}|^2 d^3\boldsymbol{r}}{\int \varepsilon_r|\boldsymbol{E}|^2 d^3\boldsymbol{r}}. \quad \text{(B5)}$$

The thermal Langevin source $F(\boldsymbol{r},t)$ exhibits the following statistics in the frequency domain [1]

$$\begin{aligned}&\langle\tilde{F}(\boldsymbol{k},\omega)\tilde{F}^*(\boldsymbol{k}',\omega')\rangle\\&=(2\pi)^4\frac{2D_Tk_BT_0^2}{\rho C}|\boldsymbol{k}|^2\delta(\boldsymbol{k}-\boldsymbol{k}')\delta(\omega-\omega'),\end{aligned}\tag{B6}$$

where $\tilde{F}(\boldsymbol{k},\omega)$ is the Fourier transform of $F(\boldsymbol{r},t)$, $k_B$ is the Boltzmann constant, and $T_0$ is the device temperature at thermal equilibrium. Accordingly, the corresponding statistics in the real space is given by

$$\begin{aligned}&\langle F(\boldsymbol{r}_1,t_1)F(\boldsymbol{r}_2,t_2)\rangle\\&=\frac{2D_Tk_BT_0^2}{\rho C}\delta(t_1-t_2)\nabla_{\boldsymbol{r}_1}\cdot\nabla_{\boldsymbol{r}_2}[\delta(\boldsymbol{r}_1-\boldsymbol{r}_2)],\end{aligned}\tag{B7}$$

where $\nabla_{\boldsymbol{r}_j}$ $(j=1,2)$ denotes gradient over $\boldsymbol{r}_j$. As a result, the mode-averaged thermal source $\xi(t)$ exhibits the following statistics

$$\begin{aligned}\langle\xi(t)\xi(t+\tau)\rangle&=\frac{2D_Tk_BT_0^2}{\rho C}\frac{\int|\nabla(\varepsilon_r|\boldsymbol{E}|^2)|^2d^3\boldsymbol{r}}{(\int\varepsilon_r|\boldsymbol{E}|^2d^3\boldsymbol{r})^2}\delta(\tau)\\&\equiv S_\xi\delta(\tau).\end{aligned}\tag{B8}$$

On the other hand, as the thermal diffusion transfers the heat to surrounding areas which reduces the magnitude of temperature variation, the second term of Eq. (B3) can be well approximated by a thermal relaxation term as [14, 57]

$$\frac{\int D_T\nabla^2(\Delta T)\varepsilon_r|\boldsymbol{E}|^2d^3\boldsymbol{r}}{\int\varepsilon_r|\boldsymbol{E}|^2d^3\boldsymbol{r}}=-\Gamma_T\Delta\bar{T},\tag{B9}$$

where $\Gamma_T$ represents the thermal relaxation rate. Although the exact behavior of thermal diffusion in a device depends on the specific boundary conditions of the device [1, 2, 10, 11], the simple thermal relaxation given by Eq. (B9) provides an excellent description of thermodynamics in various microresonators [14, 16–22, 24–27, 57]. Therefore, Eq. (B3) becomes

$$\frac{d(\Delta\bar{T})}{dt}=-\Gamma_T\Delta\bar{T}+\eta_TU_o+\xi(t),\tag{B10}$$

where $U_o=|a|^2$ is the optical energy inside the cavity. Equation (B10) is Eq. (2) in the main text.

In the absence of photothermal heating, Eq. (B10) results in $\langle(\Delta\bar{T})^2\rangle=\frac{S_\xi}{2\Gamma_T}$. As thermodynamics [28] requires the temperature fluctuation to be $\langle(\Delta\bar{T})^2\rangle=\frac{k_BT_0^2}{\rho CV}$, where $V$ is the effective mode volume, it infers that

$$S_\xi=\frac{2\Gamma_Tk_BT_0^2}{\rho CV},\tag{B11}$$

which is expected from the fluctuation-dissipation of the system. Compare Eq. (B11) with Eq. (B8), we can find the thermal relaxation rate is related to the device parameter as

$$\Gamma_T=D_TV\frac{\int|\nabla(\varepsilon_r|\boldsymbol{E}|^2)|^2d^3\boldsymbol{r}}{(\int\varepsilon_r|\boldsymbol{E}|^2d^3\boldsymbol{r})^2}.\tag{B12}$$

### Appendix C: Spectrum of temperature fluctuations

Assume that a continuous-wave (CW) laser is launched into the cavity. The photothermal effect would heat the device, leading to a static temperature change of $\Delta\bar{T}_0$. As a result, the temperature variation consists of both the fundamental thermal fluctuations and the static temperature rise induced by photothermal heating, which can be written as $\Delta\bar{T}=\Delta\bar{T}_0+\delta\bar{T}(t)$. Accordingly, the cavity field becomes $a=a_0+\delta a(t)$ where $a_0$ is the cavity field under the impact of static temperature rise $\Delta\bar{T}_0$ and $\delta a(t)$ represents the field fluctuation induced by the temperature fluctuations. From Eqs. (1) and (2) of the main text, we can find that $\Delta\bar{T}_0$ and $a_0$ satisfy the following equations

$$\frac{da_0}{dt}=(i\Delta_0-ig_T\Delta\bar{T}_0-\Gamma_t/2)a_0+i\sqrt{\Gamma_e}A,\tag{C1}$$

$$\frac{d(\Delta\bar{T}_0)}{dt}=-\Gamma_T\Delta\bar{T}_0+\eta_T|a_0|^2,\tag{C2}$$

which result in $\Delta\bar{T}_0$ and $a_0$ given as

$$\Delta\bar{T}_0=\frac{\eta_T}{\Gamma_T}|a_0|^2,\qquad a_0=\frac{i\sqrt{\Gamma_e}A}{\Gamma_t/2-i\Delta_0'},\tag{C3}$$

where $\Delta_0'\equiv\Delta_0-g_T\Delta\bar{T}_0=\Delta_0-g_T\eta_T|a_0|^2/\Gamma_T$. The mode-averaged temperature thus increases to $\bar{T}_0'=T_0+\Delta\bar{T}_0$. Consequently, Eq. (B11) becomes

$$S_\xi=\frac{2\Gamma_Tk_B(T_0+\Delta\bar{T}_0)^2}{\rho CV}=\frac{2\Gamma_Tk_B}{\rho CV}\left(T_0+\frac{\eta_T}{\Gamma_T}|a_0|^2\right)^2.\tag{C4}$$

$\delta\bar{T}(t)$ and $\delta a(t)$ are governed by Eqs. (4) and (5) in the main text, which can be solved analytically in the frequency domain to find the spectral intensity of temperature fluctuations as

$$S_{\delta\bar{T}}(\Omega)=\frac{S_\xi}{\left|\Gamma_T-i\Omega+2\eta_Tg_T|a_0|^2\Delta_0'L_+(\Omega)L_-(\Omega)\right|^2},\tag{C5}$$

where $L_\pm(\Omega)\equiv1/[i(\Delta_0'\pm\Omega)\mp\Gamma_t/2]$ and $S_\xi$ is given by Eq. (C4). In general, the thermal relaxation rate is much smaller than the photon decay rate of the optical cavity, $\Gamma_T\ll\Gamma_t$, and the modulation frequency $\Omega$ thus falls in the regime $\Omega\ll\Gamma_t$. As a result, Eq. (C5) reduces to a simple expression given in Eq. (6) of the main text.

### Appendix D: Optimal temperature squeezing

From Eq. (9) of the main text, it is straightforward to find that the optimal temperature squeezing is achieved at an optical energy of

$$|a_0|^2=\frac{\Gamma_TT_0}{\eta_T}\frac{1-\Gamma_t\Gamma_TL_0+1/(g_TT_0\Delta_0'L_0)}{1-4g_TT_0\Gamma_T\Gamma_t\Delta_0'L_0^2},\tag{D1}$$

where $L_0\equiv1/[(\Delta_0')^2+(\Gamma_t/2)^2]$. In general, optical materials have thermo-optic coefficients in the order of $|\frac{dn}{dT}|\sim10^{-5}/K$

[39]. For a device at room temperature, $|g_T T_0| \sim \frac{\omega_0}{10^3}$ which is much larger than $\Gamma_t$ for a device with a loaded optical $Q_t \gg 10^3$. As a result, $g_T T_0 \Delta_0' L_0 \gg 1$. On the other hand, as discussed previously, the thermal relaxation rate is much smaller than the photon decay rate of the optical cavity, $\Gamma_T \ll \Gamma_t$, which leads to $\Gamma_t \Gamma_T L_0 \ll 1$. Consequently, Eq. (D1) is well approximated by

$$|a_0|^2 \approx \frac{\Gamma_T T_0/\eta_T}{1-4g_T T_0 \Gamma_T \Gamma_t \Delta_0' L_0^2}. \tag{D2}$$

Substitute this expression into Eq. (9) of the main text and use the same conditions $g_T T_0 \Delta_0' L_0 \gg 1$ and $\Gamma_t \Gamma_T L_0 \ll 1$, we can find the optimal temperature squeezing is given by

$$\mathscr{F}_o \approx 4\Gamma_T \Gamma_t L_0 - \frac{2}{g_T T_0 \Delta_0' L_0}, \tag{D3}$$

At the optimal laser-cavity detuning of $\Delta_0' = \Gamma_t/2$, Eqs. (D2) and (D3) become

$$\mathscr{F}_o \approx \frac{8\Gamma_T}{\Gamma_t} + \frac{2\Gamma_t}{|g_T|T_0}, \tag{D4}$$

$$|a_0|^2 \approx \frac{\Gamma_T T_0/\eta_T}{1+8|g_T|T_0 \Gamma_T/\Gamma_t^2}, \tag{D5}$$

which are Eqs. (10) and (11) of the main text.

### Appendix E: Theory of the impact of laser noises

A CW laser exhibits fundamental fluctuation on its power and/or phase which would perturb device temperature via photothermal heating. To thoroughly describe such effect, we treat the optical field quantum mechanically. The device temperature, however, is a thermodynamic parameter and is well described as a classical variable. The Hamiltonian of the optical cavity system is given by

$$\mathscr{H} = \hbar\omega_0'(\bar{T}) a^\dagger a - \hbar\sqrt{\Gamma_e}\left[a^\dagger A e^{-i\omega_l t} + A^\dagger a e^{i\omega_l t}\right], \tag{E1}$$

where $\omega_0'(\bar{T}) = \omega_0 + g_T \Delta\bar{T}$ as described in the previous section. For convenience, in Eq. (E1), the intracavity field operator $a$ is now normalized such that $a^\dagger a$ represents the photon number operator and $A$ is the field operator of the incoming wave at carrier frequency $\omega_l$ inside the coupling waveguide normalized such that $A^\dagger A$ represents the operator of the input photon flux.

Using Eq. (E1) and counting in the intrinsic cavity loss [58], we obtain the following equation of motion in the Heisenberg picture governing the wave dynamics inside the cavity:

$$\frac{da}{dt} = (i\Delta_0 - \Gamma_t/2)a - ig_T \Delta\bar{T} a + i\sqrt{\Gamma_e} A + i\sqrt{\Gamma_0} u, \tag{E2}$$

where $\Gamma_0$ is the photon decay rate of the intrinsic cavity, which is related to the loaded cavity as and $\Gamma_t = \Gamma_0 + \Gamma_e$. $u$ is the noise operator associated with intrinsic cavity loss, which satisfies the commutation relation of $[u(t), u^\dagger(t')] = \delta(t-t')$. For convenience, in Eq. (E2), we have made a transform $a \to a e^{-i\omega_l t}$ to remove the laser carrier $e^{-i\omega_l t}$. The dynamics of the mode-averaged temperature fluctuation $\Delta\bar{T}$ is governed by Eq. (B10) where the optical energy $U_o$ is now given by $U_o = \hbar\omega_0 a^\dagger a$.

In general, the input CW laser is accompanied with classical noises on its intensity and phase and the fundamental quantum fluctuation of the optical field. To describe the fluctuations of the input laser, the input CW wave can be treated as a classical field with a constant amplitude of $A_0$, accompanied with two fluctuation terms: $A(t) = A_0 + A_c(t) + A_Q(t)$, where $A_c(t)$ stands for the classical noises (in both intensity and phase) and $A_Q(t)$ represents the quantum fluctuation. $A_Q(t)$ satisfies the commutation relation of $[A_Q(t), A_Q^\dagger(t')] = \delta(t-t')$. The classical noise term $A_c(t)$ consists of both intensity and phase noises: $A_c(t) = A_0[\frac{1}{2} f_P(t) + i\delta\phi(t)]$ where $f_P(t) \equiv \frac{\delta P(t)}{P}$ is the relative intensity noise with a spectral density given by $S_{\mathrm{RIN}}(\Omega)$, and $P = \hbar\omega_0 |A_0|^2$ stands for the input laser power. $\delta\phi(t)$ represents the phase fluctuation of the input laser, with a spectral density given by $\frac{S_\omega(\Omega)}{\Omega^2}$ where $S_\omega(\Omega)$ is the spectral intensity of the laser frequency noises. Therefore, $A_c(t)$ exhibits a spectral density given as

$$S_{A_c}(\Omega) = |A_0|^2 \left[\frac{1}{4} S_{\mathrm{RIN}}(\Omega) + \frac{1}{\Omega^2} S_\omega(\Omega)\right], \tag{E3}$$

where, for simplicity, we have assumed the laser intensity noise and frequency noise are independent with each other.

Similar to the previous section, the intracavity optical field and the temperature fluctuation each can be separated into a static term and a fluctuation term, $a = a_0 + \delta a(t)$ and $\Delta\bar{T} = \Delta\bar{T}_0 + \delta\bar{T}(t)$. $\Delta\bar{T}_0$ and $a_0$ are given by Eq. (C3) (where $|a_0|^2$ is now replaced by $\hbar\omega_0|a_0|^2$ due to the different field normalization used in this section and $A$ is replaced by $A_0$ because of the notation change). $\delta\bar{T}(t)$ and $\delta a(t)$ are now governed by the following equations which includes both the classical and quantum fluctuations of the optical field

$$\begin{aligned}\frac{d(\delta a)}{dt} =\ & (i\Delta_0' - \Gamma_t/2)\delta a - ig_T a_0 \delta\bar{T} + i\sqrt{\Gamma_e} A_c \\ & + i\sqrt{\Gamma_e} A_Q + i\sqrt{\Gamma_0} u, \end{aligned} \tag{E4}$$

$$\frac{d(\delta\bar{T})}{dt} = -\Gamma_T \delta\bar{T} + \eta_T \hbar\omega_0 (a_0^* \delta a + a_0 \delta a^\dagger) + \xi(t). \tag{E5}$$

These two equations can be solved analytically in the frequency domain to obtain the spectral intensity of temperature fluctuations as

$$\begin{aligned} S_{\delta\bar{T}}(\Omega) &= \frac{S_\xi + S_Q + S_L}{\left|\Gamma_t - i\Omega + 2\eta_T g_T U_o \Delta_0' L_+(\Omega) L_-(\Omega)\right|^2} \\ &\approx \frac{S_\xi + S_Q + S_L}{(\Gamma_T')^2 + (\kappa_T \Omega)^2}, \end{aligned} \tag{E6}$$

where $U_o = \hbar\omega_0 |a_0|^2$ is the optical energy inside the cavity, $\Gamma_T'$ and $\kappa_T$ are given by Eqs. (7) and (8) in the main text, and $S_\xi$ is given in Eq. (C4). Equation (E6) is Eq. (14) in the main text.

In Eq. (E6), $S_Q$ describes the effect of quantum backaction from the quantum fluctuations of the input laser, which

is given by

$$S_Q(\Omega) = \eta_T^2 \hbar\omega_0 U_o \Gamma_t |L_-(\Omega)|^2 \approx \frac{\eta_T^2 \hbar\omega_0 U_o \Gamma_t}{(\Delta_0')^2 + (\Gamma_t/2)^2}, \quad \text{(E7)}$$

which is Eq. (16) in the main text. $S_L$ describes the effect of the classical noises accompanied with the input laser, which is given by

$$\begin{aligned} S_L(\Omega) = \; & \eta_T^2 U_o^2 |L_+(\Omega) L_-(\Omega)|^2 \left\{ S_{\rm RIN}(\Omega)[(\Omega\Gamma_t/2)^2 + 1/L_0^2] \right. \\ & \left. + (2\Delta_0')^2 S_\omega(\Omega) \right\} \\ \approx \; & \eta_T^2 U_o^2 \left\{ S_{\rm RIN}(\Omega) + \frac{(2\Delta_0')^2 S_\omega(\Omega)}{[(\Delta_0')^2 + (\Gamma_t/2)^2]^2} \right\}, \end{aligned} \quad \text{(E8)}$$

which is Eq. (17) in the main text.

Equations (E6)-(E8) provide a complete description of the temperature spectrum under the impact of photothermal backaction, quantum backaction, and the laser classical noises.

### Appendix F: The thermo-elastic coupling

The same theory can be applied to describe the thermo-elastic effect [1, 11, 12]. In this case, the temperature fluctuations of the device change the geometry and boundary of the device through thermal expansion, which in turn perturb the cavity resonance by an amount given by [54]

$$\begin{aligned} \delta\omega &= -\frac{\omega_0}{2} \frac{\int \frac{dh}{dT} \Delta T(\boldsymbol{r}) \left[ \Delta\varepsilon_r |\boldsymbol{E}_\parallel|^2 - \Delta(\varepsilon_r^{-1}) |\boldsymbol{D}_\perp|^2 \right] dA}{\int \varepsilon_r |\boldsymbol{E}|^2 d^3\boldsymbol{r}} \\ &= -\frac{\omega_0}{2} \frac{1}{h} \frac{dh}{dT} \frac{\int h(\boldsymbol{r}) \Delta T(\boldsymbol{r}) \left[ \Delta\varepsilon_r |\boldsymbol{E}_\parallel|^2 - \Delta(\varepsilon_r^{-1}) |\boldsymbol{D}_\perp|^2 \right] dA}{\int \varepsilon_r |\boldsymbol{E}|^2 d^3\boldsymbol{r}}, \end{aligned} \quad \text{(F1)}$$

where the integration in the numerator $\int dA$ is over the device boundary [54]. $\frac{1}{h}\frac{dh}{dT}$ is the linear thermal expansion coefficient of the device which is assumed to be uniform around the device broundary. Therefore, the thermo-elastic perturbation to the cavity resonance can be written as $\delta\omega = g_T \Delta\bar{T}$, where the photothermal coupling coefficient is now given as $g_T \equiv \frac{d\omega_0}{dT} = -\frac{\omega_0}{2h}\frac{dh}{dT}$ and the mode-averaged temperature variation is given by

$$\Delta\bar{T} \equiv \frac{\int h(\boldsymbol{r}) \Delta T(\boldsymbol{r}) \left[ \Delta\varepsilon_r |\boldsymbol{E}_\parallel|^2 - \Delta(\varepsilon_r^{-1}) |\boldsymbol{D}_\perp|^2 \right] dA}{\int \varepsilon_r |\boldsymbol{E}|^2 d^3\boldsymbol{r}}. \quad \text{(F2)}$$

Following a similar procedure as Section II, we can find the dynamics of $\Delta\bar{T}$ is governed by an equation with a same form of Eq. (B10) while the photothermal heating coefficient $\eta_T$, the thermal relaxation rate $\Gamma_T$, and the mode-averaged Langiven thermal source $\xi(t)$ have different values from the thermo-optic case. Therefore, we expect that the photothermal temperature squeezing would behave in a similar manner for the thermo-elastic effect.


[1] V. B. Braginsky, M. L. Gorodetsky, and S. P. Vyatchanin, Phys. Lett. A **264**, 1 (1999).
[2] V. B. Braginsky, M. L. Gorodetsky, and S. P. Vyatchanin, Phys. Lett. A **271**, 303 (2000).
[3] K. Numata, A. Kemery, and J. Camp, Phys. Rev. Lett. **93**, 250602 (2004).
[4] M. Evans, S. Ballmer, M. Fejer, P. Fritschel, G. Harry, and G. Ogin, Phys. Rev. D **78**, 102003 (2008).
[5] K. Goda, K. McKenzie, E. E. Mikhailov, P. K. Lam, D. E. McClelland, and N. Mavalvala, Phys. Rev. A **72**, 043819 (2005).
[6] M. R. Foreman, J. D. Swaim, and F. Vollmer, Adv. Opt. Photon. **7**, 168 (2015).
[7] F. Vollmer and S. Arnold, Nature Methods **5**, 591 (2008).
[8] X. Fan, I. M. White, S. I. Shopova, H. Zhu, J. D. Suter, and Y. Sun, Anal. Chem. ACTA **620**, 8 (2008).
[9] M. Aspelmeyer, T. J. Kippenberg, and F. Marquardt, Rev. Mod. Phys. **86**, 1391 (2014).
[10] M. L. Gorodetsky and I. S. Grudinin, J. Opt. Soc. Am. B **21**, 697 (2004).
[11] A. B. Matsko, A. A. Savchenkov, N. Yu, and L. Maleki, J. Opt. Soc. Am. B **24**, 1324 (2007).
[12] A. A. Savchenkov, A. B. Matsko, V. S. Ilchenko, N. Yu, and L. Maleki, J. Opt. Soc. Am. B **24**, 2988 (2007).
[13] A. E. Fomin, M. L. Gorodetsky, I. S. Grudinin, and V. S. Ilchenko, J. Opt. Soc. Am. B **22**, 459 (2005).
[14] T. Carmon, L. Yang, and K. J. Vahala, Opt. Express **12**, 4742 (2004).
[15] T. J. Johnson, M. Borselli, and O. Painter, Opt. Express **14**, 817 (2005).
[16] W.-S. Park and H. Wang, Opt. Lett. **32**, 3104 (2007).
[17] C. Schmidt, A. Chipouline, T. Pertsch, A. Tünnermann, O. Egorov, F. Lederer, and L. Deych, Opt. Express **16**, 6285 (2008).
[18] L. He, Y.-F. Xiao, J. Zhu, S. K. Ozdemir, and L. Yang, Opt. Express **17**, 9571 (2009).
[19] M. W. Lee, *et al*, Opt. Express **18**, 26695 (2010).
[20] M. Brunstein, A. M. Yacomotti, I. Sagnes, F. Raineri, L. Bigot, and A. Levenson, Phys. Rev. A **85**, 031803(R) (2012).
[21] C. Baker, S. Stapfner, D. Parrain, S. Ducci, G. Leo, E. M. Weig, and Ivan Favero, Opt. Express **20**, 29076 (2012).
[22] J. Li, S. Diddams, and K. J. Vahala, Opt. Express **22**, 14559 (2014).
[23] I. Teraoka, Opt. Comm. **310**, 212 (2014).
[24] D. M. Abrams, A. Slawik, and K. Srinivasan, Phys. Rev. Lett.

**112**, 123901 (2014).
[25] W. Weng, J. D. Anstie, P. Abbott, B. Fan, T. M. Stace, and A. N. Luiten, Phys. Rev. A **91**, 063801 (2015).
[26] Q. Wang, Y. Wang, Z. Guo, J. Wu, and Y. Wu, Opt. Lett. **40**, 1607 (2015).
[27] S. Diallo, G. Lin, and Y. K. Chembo, Opt. Lett. **40**, 3834 (2015).
[28] L. D. Landau and E. M. Lifshitz, *Statistical Physics*, 3rd Ed., Course of Theoretical Physics, Vol. 5 (Pergamon Press, 1980).
[29] D. K. Armani, T. J. Kippenberg, S. M. Spillane, and K. J. Vahala, Nature **421**, 925 (2003).
[30] T. Ioppolo, U. Ayaz, and M. V. Ötügen, Opt. Express **17**, 16465 (2009).
[31] N. A. Yebo, P. Lommens, Z. Hens, and R. Baets, Opt. Express **18**, 11859 (2010).
[32] A. G. Krause, M. Winger, T. D. Blasius, Q. Lin, and O. Painter, Nature Photon. **6**, 768 (2012).
[33] C. Ciminelli, F. Dell'Olio, C. E. Campenella, and M. N. Armenise, Adv. Opt. Photon. **2**, 370 (2010).
[34] M. R. Foreman, and F. Vollmer, Phys. Rev. Lett. **114**, 118001 (2015).
[35] I. M. White and X. Fan, Opt. Express **16**, 1020 (2008).
[36] J. D. Swaim, J. Knittle, and W. P. Bowen, Appl. Phys. Lett. **99**, 243109 (2011).
[37] M. R. Foreman, W.-L. Jin, and F. Vollmer, Opt. Express **22**, 5491 (2014).
[38] J. Alnis, A. Schliesser, C. Y. Wang, J. Hofer, T. J. Kippenberg, and T. W. Hänsch, Phys. Rev. A **84**, 011804(R) (2011).
[39] M. Bass, Ed, *Handbook of Optics*, 3rd Ed., Vol. IV (Optical Society of America, 2010).
[40] M. Maldovan, Nature **503**, 209 (2013); Nature Mat. **14**, 667 (2015).
[41] G. P. Agrawal, *Lightwave Technology: Components and Devices* (Wiley, 2004).
[42] T. Nazarova, C. Lisdat, F. Riehle, and U. Sterr, J. Opt. Soc. Am. B **25**, 1632 (2008).
[43] F. Kéfélian, H. Jiang, P. Lemonde, and G. Santarelli, Opt. Lett. **34**, 914 (2009).
[44] Q. Lin, M. A. Van Camp, H. Zhang, B. Jelekovic, and V. Vuletic, Opt. Lett. **37**, 1989 (2012).
[45] S. S. Sane, S. Bennetts, J. E. Debs, C. C. N. Kuhn, G. D. McDonald, P. A. Altin, J. D. Close, and N. P. Robins, Opt. Express **20**, 8915 (2012).
[46] J. Dong, Y. Hu, J. Huang, M. Ye, Q. Qu, T. Li, and L. Liu, Appl. Opt. **54**, 1152 (2015).
[47] R. Smid, M. Cizek, B. Mikel, and O. Cip, Sensors **15**, 1342 (2015).
[48] A. S. Rury, K. Mansour, and N. Yu, Appl. Phys. B **120**, 155 (2015).
[49] W. Liang, V. S. Ilchenko, D. Eliyahu, A. A. Savchenkov, A. B. Matsko, D. Seidel, and L. Maleki, Nature Comm. **6**, 7371 (2015).
[50] U. Sterr, T. Legero, T. Kessler, H. Schnatz, G. Grosche, O. Terra, and F. Riehle, Proc. SPIE, Time and Frequency Metrology II, Vol. 7431, 74310A (2016).
[51] For example, Redfern Integrated Optics (RIO)-OptaSense Inc.: http://www.rio-inc.com/; NKT Photonics: http://www.nktphotonics.com/.
[52] T. J. Kippenberg, R. Holzwarth, S. A. Diddams, Science **332**, 555 (2011).
[53] A. Dutt, K. Luke, S. Manipatruni, A. L. Gaeta, P. Nussenzveig, and M. Lipson, Phys. Rev. Appl. **3**, 044005 (2015).
[54] S. G. Johnson, M. Ibanescu, M. A. Skorobogatiy, O. Weisberg, J. D. Joannopoulos, Phys. Rev. E **65**, 066611 (2002).
[55] J. Bravo-Abad, S. Fan, S. G. Johnson, J. D. Joannopoulos, and M. Soljačič, J. Lightwave Technol. **25**, 2539 (2007).
[56] H. A. Haus, *Waves and Fields in Optoelectronics* (Prentice-Hall, Englewood Cliffs, N.J., 1984).
[57] T. J. Johnson, M. Borselli, and O. Painter, Opt. Express **14**, 817 (2006).
[58] Walls, D. F. & Milburn, G. J. Quantum Optics. 2nd Ed. (Springer, 2008).